Colloquia: LaThuile11

Early pp physics at ALICE

E. Scomparin for the ALICE Collaboration

INFN, Sezione di Torino - Torino, Italy

Summary. — The ALICE experiment, dedicated for heavy-ion collisions at the LHC, is taking data with proton-proton collisions since November 2009. This contribution summarizes the first year of operation and performance of the ALICE detector at the LHC as well as the first results from pp collisions at 0.9 TeV and 7 TeV. In particular, results on global event properties and identified particle spectra, including strangeness, open charm and charmonium production, will be discussed.

PACS `12.38.-t` – Quantum chromodynamics.
PACS `12.38.Mh` – Quark-gluon plasma.

1. – Introduction

The ALICE detector is very different in both design and purpose from the other experiments at the CERN Large Hadron Collider (LHC). Its main aim is the study of matter under extreme conditions of temperature and pressure, *i.e.* the Quark-Gluon Plasma (QGP), in collisions between heavy ions. With an energy up to almost 30 times higher than that of RHIC, the BNL heavy-ion collider, a very different type of QGP, in terms of initial temperature, lifetime and system volume can be formed at the LHC. Furthermore, for the first time, a conspicuous production of hard signals like jets and heavy quarks which serve as probes to study QGP properties can be observed. Data taking with proton-proton collisions is very important for ALICE, primarily to collect comparison data for the heavy-ion programme. Therefore, our goal in 2010 was to collect about 10^9 Minimum-Bias (MB) pp collisions, to provide sufficient comparison statistics for the first heavy-ion run which took place in November-December 2010. However, given the specific capabilities of the ALICE detector, complementary to those of the other LHC experiments, a number of measurements concerning soft and semi-hard QCD processes are of interest on their own in pp collisions, and are part of the physics programme [1]. More in detail, the large MB pp sample was used to provide a detailed characterization of global event properties over a range of LHC energies, which can be very useful for tuning Monte Carlo generators to better describe the QCD background underlying searches for new physics. Furthermore, results on identified particles, including strange mesons and baryons, open charm and charmonium, were also obtained.

The very first proton-proton collisions in the ALICE intersection region occurred on 23rd November 2009, at a centre-of-mass energy $\sqrt{s} = 0.9$ TeV, during the commissioning of the accelerator. The first few hundreds of recorded pp events served to measure the charged-particle pseudorapidity density in these collisions [2], the first published result obtained with particle collisions at the LHC. At the end of the 2009 commissioning run, the LHC achieved the highest energy of $\sqrt{s} = 2.36$ TeV, at which ALICE collected data on a few 10^4 pp collisions. After the winter shutdown, the LHC running resumed in March 2010 at the collision energy of $\sqrt{s} = 7$ TeV. During 2010, ALICE has collected at this energy more than 8×10^8 MB triggers and about 1.3×10^8 muon triggers, the latter corresponding to an integrated luminosity larger than $100 \, \text{nb}^{-1}$. In ALICE, the MB trigger corresponds to the detection of a charged particle in the most central 5 η-units, while a muon trigger requires, in addition, the detection of a particle in the forward muon spectrometer covering the region $2.5 < \eta < 4$.

The first data taking with Pb-Pb collisions took place at the end of 2010. A summary of the first results can be found in [3].

2. – Detector

The ALICE detector consists of a central part, which measures hadrons, electrons and photons, and a forward spectrometer to measure muons. The central part, which covers the pseudorapidity range $|\eta| < 1$ over the full azimuth, is embedded in the large L3 solenoidal magnet supplying a field of 0.5 T. This part consists of: an Inner Tracking System (ITS) of high-resolution silicon detectors; a cylindrical Time-Projection Chamber (TPC); three particle-identification arrays of Time-Of-Flight (TOF), Transition-Radiation-Detector (TRD), and Čerenkov-ring-imaging (called HMPID) counters; two single-arm electromagnetic calorimeters (high resolution PHOS and large acceptance EMCAL). The forward muon spectrometer covering $-4 < \eta < -2.5$ consists of an arrangement of hadron absorbers, a large dipole magnet with a field integral of 3 Tm, and 14 stations of tracking and triggering chambers. Several smaller detectors for triggering and multiplicity measurements (VZERO, T0, FMD, PMD, ZDC) are located at small angles. The main design features include: a robust and redundant, but limited-pseudorapidity-acceptance tracking, designed to cope with the very high particle density in nuclear collisions; a minimum of material in the sensitive tracking volume (10% of radiation length between interaction point and outer radius of the TPC) to reduce multiple scattering; several detector subsystems dedicated to particle identification over a large range in momentum. The layout of the ALICE detector and its eighteen different subsystems are described in detail in [4]. The experiment is essentially fully installed, commissioned and operational. Two subsystems (TRD and EMCAL) which were added more recently in the experiment, had, for the 2010 run, about 40% of their active area installed and will be completed for the next runs. The many years of preparation, analysis tuning with simulations, and detector commissioning with cosmic rays during much of 2008-2009 resulted in having most of the detector components working with collisions rather close to performance specifications. As an example of the performance, the energy-loss distribution in the TPC is shown in fig. 1 (left panel) as a function of momentum, demonstrating the clear separation between particle species reached in the non-relativistic momentum region. After careful calibration with radioactive krypton injected into the gas volume and with cosmic-ray data, the energy loss resolution is about 5–6%, corresponding to design value. To demonstrate, as another example, the TOF performance, in fig. 2 (right panel) the particle velocity β is shown as a function of the rigidity, separately for positive
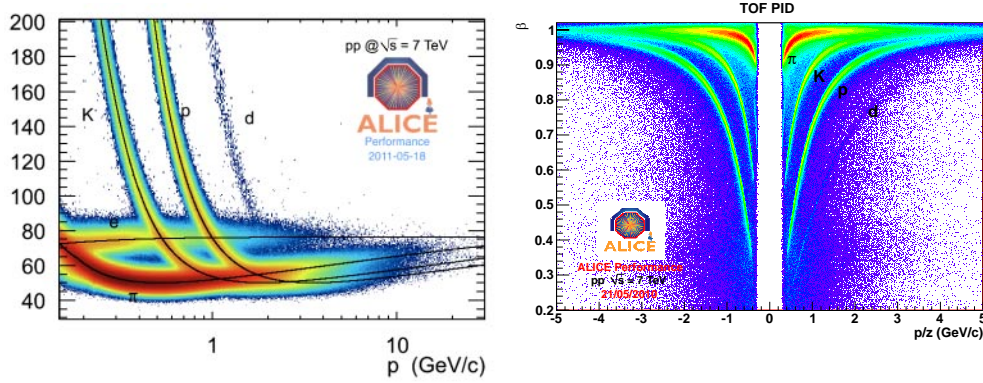
Fig. 1. – Left: dE/dx spectrum *versus* momentum in the ALICE TPC for 7 TeV pp collisions. The lines are a parameterization of the Bethe-Bloch curve. Right: Particle velocity β measured with TOF, as a function of momentum.

and negative charges. The inferred time resolution of the TOF detector is about 90 ps, very close to its design specification.

3. – Physics results

At the time of this conference, a large number of physics results have already been obtained, and only a few of them, for reasons of space, can be shortly summarized in this contribution.

The charged-particle pseudorapidity density $dN_{\rm ch}/d\eta$ as well as the multiplicity distributions were measured at 0.9 TeV, 2.36 TeV and 7 TeV at mid-rapidity [2,5,6]. The energy dependence of the multiplicity density, shown in fig. 2 (left panel), is well described
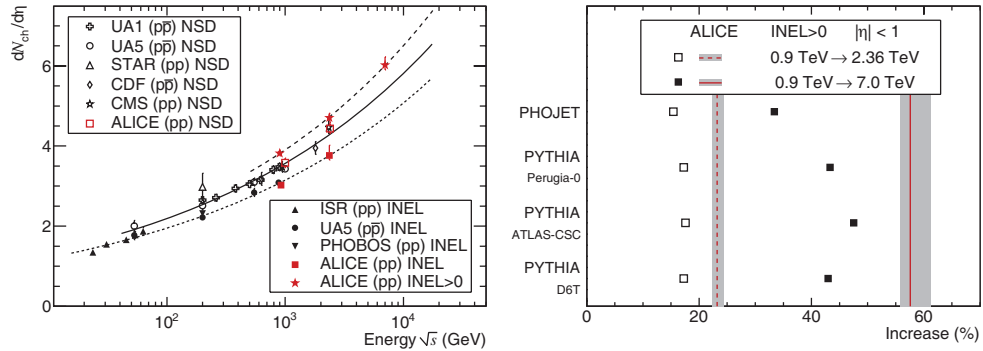

Fig. 2. – Left: Energy dependence of the charged-particle pseudorapidity density in $\eta < 0.5$ for different event classes. The lines indicate the power-law dependence, $s^{0.11}$, for non-single-diffractive events (solid line), for inelastic events (dotted line), and for inelastic events with at least one charged track in $|\eta| < 1$ (dashed line). The references for the data from other experiments can be found in [6]. Right: The relative increase of the charged-particle pseudorapidity density at $\sqrt{s} = 2.36$ TeV (dashed line) and at $\sqrt{s} = 7$ TeV (solid line) with respect to the value at $\sqrt{s} = 0.9$ TeV, compared to model predictions (see [6] for details).
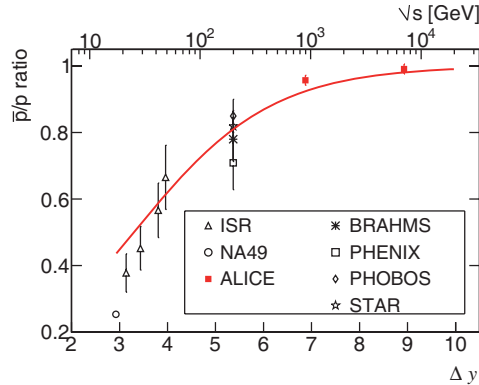
Fig. 3. – Mid-rapidity antiproton-to-proton ratio as a function of the rapidity interval Δy (lower axis) and centre-of-mass energy (upper axis). The line represents a simple calculation of this dependence, assuming Reggeon-like string-junction exchange. The references for the data from other experiments and for models can be found in [8].

by a power law in energy, and this increase is significantly stronger than that predicted by most event generators (fig. 2, right panel). Most of this stronger increase happens in the tail of the multiplicity distribution, *i.e.* for events with much larger than average multiplicity. Likewise, neither the transverse momentum distribution at 0.9 TeV, nor the dependence of average p_T on multiplicity, is well described by various versions of event generators [7], in particular when including low-momentum particles ($p_T < 0.5\,\mathrm{GeV}/c$). The shape of the p_T spectra for different multiplicity classes is very similar below $1\,\mathrm{GeV}/c$ (which includes most of the produced particles), whereas the power-law tail of these p_T spectra (above $1\,\mathrm{GeV}/c$) is significantly steeper for low-multiplicity events than for those with high multiplicities.

The LHC, by far the highest energy proton-proton collider, is well suited to study baryon-number transport over very large rapidity intervals by measuring the antiproton-to-proton ratio at mid-rapidity [8] ($\Delta y = 8.92$ at $\sqrt{s} = 7$ TeV) in order to discriminate between various theoretical models of baryon stopping. An asymmetry in proton-antiproton production at mid-rapidity can be caused by baryon-number transfer from the incoming proton. Baryon number is carried by a non-perturbative configuration of gluon fields called string junction [9], where the three strings coming from the valence quarks of a baryon join. The antiproton-to-proton ratio, shown in fig. 3, is found to be compatible with unity at $\sqrt{s} = 7$ TeV and 4% below 1 at $\sqrt{s} = 0.9$ TeV, with an experimental uncertainty of about 1.4%, dominated by the systematic error. This result favours models which predict a strong suppression of baryon-number transport over large rapidity intervals; they agree very well with standard event generators but not with those which have implemented an enhanced baryon number transport.

Strangeness production has been studied already in the first sample of pp collisions collected at the LHC, at $\sqrt{s} = 0.9$ TeV. The results include yields and transverse momentum spectra of mesons containing strange quarks (K_S^0, ϕ) and singly/doubly strange baryons (Λ, $\overline{\Lambda}$, $\Xi + \overline{\Xi}$). The results can be compared with predictions for identified particle spectra from QCD-inspired models and provide a baseline for comparisons with both pp measurements at higher energies and heavy-ion collisions. For all species the transverse momentum spectra are found to be slightly harder (*i.e.* they have a slower
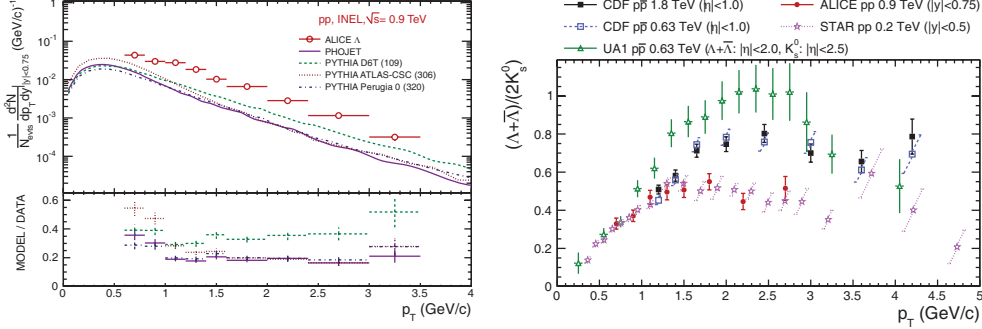
Fig. 4. – Left: Comparison of the transverse momentum differential yield for the Λ particles for pp collisions at $\sqrt{s} = 0.9$ TeV with PHOJET and several PYTHIA tunes. Right: $(\Lambda + \overline{\Lambda})/2\mathrm{K}_S^0$ as a function of p_T for different collision energies in pp and p$\overline{\mathrm{p}}$ minimum bias events. The ALICE and STAR ratios are feed-down corrected. See [10] for details as well as for references to other experimental results.

decrease with p_T) than the models. As an example, we show in fig. 4 (left) the shape of the p_T spectra for the Λ, compared to PHOJET and to several tunes of PYTHIA. For transverse momenta larger than $\sim 1\,\mathrm{GeV}/c$, the strange particle spectra are strongly underestimated by all models, by a factor of ~ 2 for K_S^0 and even ~ 3 for hyperons. The discrepancy is smaller in the case of the ϕ.

The baryon to meson ratio as a function of p_T obtained with the $\Lambda + \overline{\Lambda}$ and K_S^0 spectra measured by ALICE is presented in fig. 4 (right). It includes the $(\Lambda + \overline{\Lambda})/2\mathrm{K}_S^0$ ratio in pp collisions at 200 GeV measured by STAR, and the ratios in p$\overline{\mathrm{p}}$ collisions at 630 GeV and 1800 GeV computed with the $\Lambda + \overline{\Lambda}$ and K_S^0 spectra published by CDF and UA1. UA1 and CDF Collaborations provide inclusive spectra. The associated ratios are therefore not feed-down corrected, unlike the ALICE and STAR ones. The acceptance windows of these experiments differ significantly: ALICE measures Λ, $\overline{\Lambda}$ and K_S^0 in $|y| < 0.75$, STAR in $|y| < 0.5$, CDF in $|\eta| < 1.0$, whereas UA1 reconstructs $\Lambda + \overline{\Lambda}$ in $|\eta| < 2.0$ and K_S^0 in $|\eta| < 2.5$. The ALICE ratio agrees very well with the STAR results in the measured p_T range, which would suggest little or no energy dependence of $(\Lambda + \overline{\Lambda})/2\mathrm{K}_S^0$. A similar conclusion can be drawn when comparing only the ratios measured by CDF at 630 GeV and 1800 GeV, although the ratio found by CDF for $p_\mathrm{T} > 1.5\,\mathrm{GeV}/c$ is higher than the one observed with ALICE and STAR. The ratio computed from UA1 spectra however shows a clear disagreement with the other measurements in an intermediate p_T range between $p_\mathrm{T} \sim 1.5\,\mathrm{GeV}/c$ and $p_\mathrm{T} \sim 3.0\,\mathrm{GeV}/c$. PYTHIA simulations show that this discrepancy cannot be attributed to the differences in the acceptance or in the colliding system (*i.e.* p$\overline{\mathrm{p}}$ instead of pp); effects related to difference between the experiments in acceptance, trigger or feed-down corrections for weak decays might play a role.

The measurement of charm cross sections is needed as baseline data for our heavy-ion programme and it is of interest for comparisons with perturbative QCD calculations. The ALICE detector can measure charm production at midrapidity down to very low momenta using various hadronic decay channels. The very good signal-to-background ratio even at low transverse momenta (down to $2\,\mathrm{GeV}/c$) is a consequence of both the use of particle identification and the excellent performance of the ITS vertex detector, which has reached an impact-parameter resolution of around $80\,\mu m$ at $p_\mathrm{T} = 1\,\mathrm{GeV}/c$.
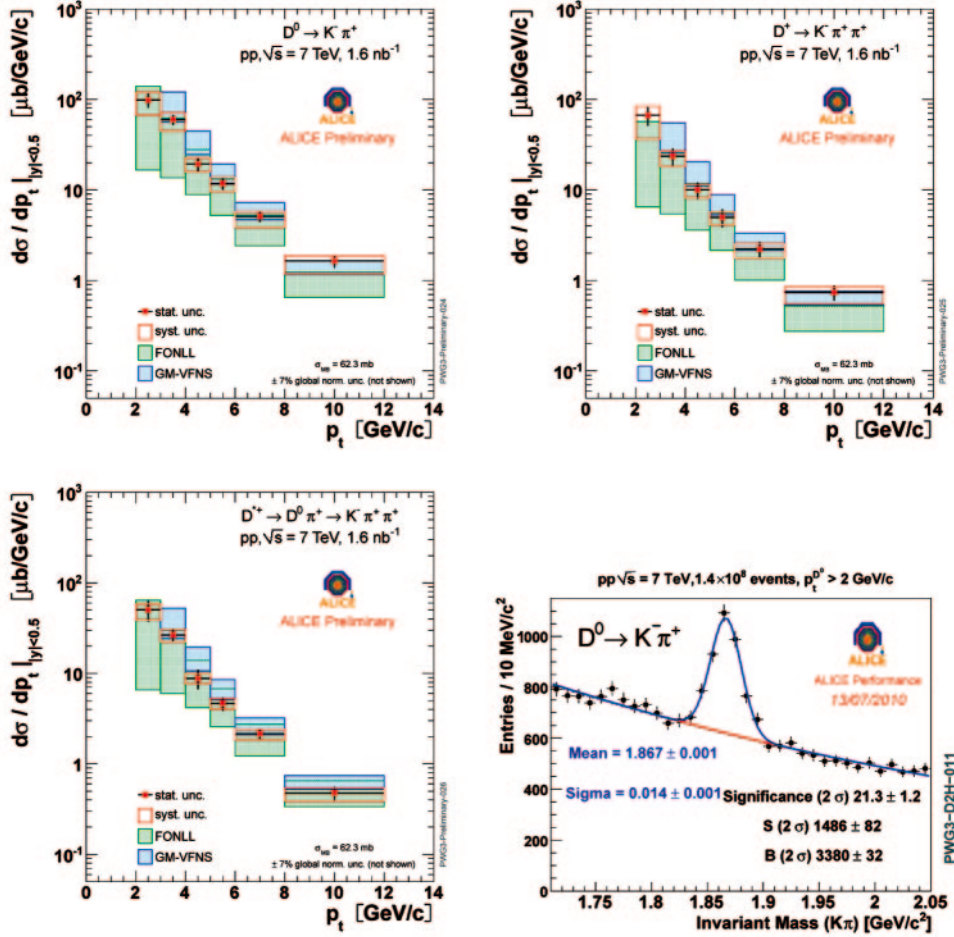
Fig. 5. – D^0, D^+, and D^{*+} p_T-differential production cross sections in $|y| < 0.5$ in pp collisions at $\sqrt{s} = 7$ TeV, compared to pQCD calculations. The p_T-integrated $D^0 \to K^- \pi^+$ signal in the $K\pi$ invariant mass distribution is also shown.

An invariant-mass analysis (see fig. 5 for an example concerning D^0) is then used to extract the raw signal yield, to be then corrected for detector acceptance and for PID, selection and reconstruction efficiency, evaluated from a detailed detector simulation. The contamination of D mesons from B meson decays is estimated to be about 15%, using the beauty production cross section predicted by the FONLL (fixed-order next-to-leading log) calculation [11] and the detector simulation, and it is subtracted from the measured raw p_T spectrum, before applying the efficiency corrections. The D^0, D^+, and D^{*+} p_T-differential production cross sections in $|y| < 0.5$ are shown in fig. 5. Theoretical predictions based on pQCD calculations (FONLL [11] and GM-VFNS [12]) are in agreement with the data.

The study of charmonium production plays an essential role in heavy-ion physics since the production of a hot, deconfined medium should lead to a suppression of $c\bar{c}$
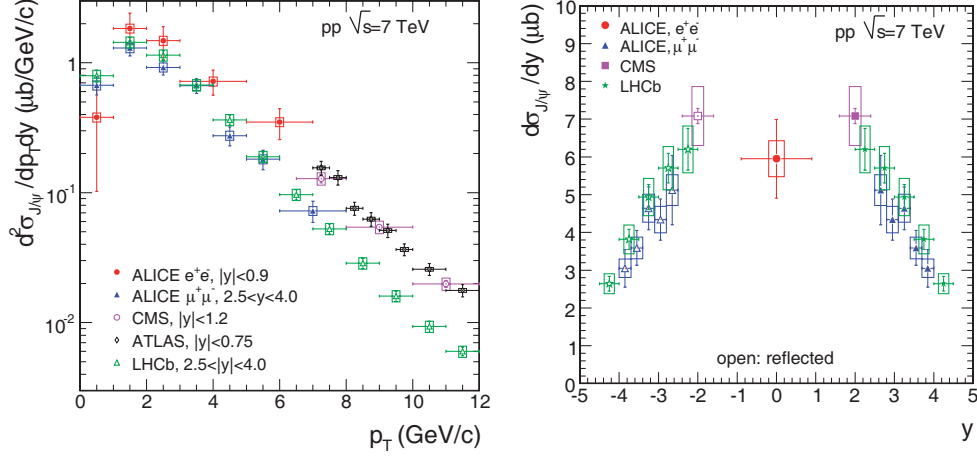
Fig. 6. – Left: $\mathrm{d}^2\sigma/\mathrm{d}p_\mathrm{T}\mathrm{d}y$ for J/ψ production in $\sqrt{s} = 7\,\mathrm{TeV}$ pp collisions. The ALICE results are compared to those from the other LHC experiments. Right: $\mathrm{d}\sigma/\mathrm{d}y$ for J/ψ production in $\sqrt{s} = 7\,\mathrm{TeV}$ pp collision. Results from other experiments are shown when their rapidity coverage extends down to $p_\mathrm{T} = 0$. See [13] for details and references to other experimental results.

bound states. A similar effect should also be visible in the bottomonium sector. As for other observables, pp reference data are essential as a baseline, and are useful to constrain theoretical models for hadro-production. In ALICE, J/ψ has been studied [13] over a large y range, including central ($|y| < 0.9$) and forward rapidity ($2.5 < y < 4$), and in both regions the transverse momentum coverage extends down to $p_\mathrm{T} = 0$. At central rapidity leptons from the $J/\psi \to e^+e^-$ decay are identified in the TPC, and the use of TOF and TRD to increase the purity of the signal is currently under study. At forward rapidity, muons from the $J/\psi \to \mu^+\mu^-$ decay are measured in the forward muon arm. In fig. 6 (left) the J/ψ transverse momentum distributions for pp collisions at $\sqrt{s} = 7\,\mathrm{TeV}$ are shown and compared with results from the other LHC experiments. The ALICE muon measurement and the LHCb result, covering the same y range, are in good agreement, while the ALICE electron result complements the high p_T ATLAS and CMS distributions, reaching $p_\mathrm{T} = 0$. In fig. 6 (right) we present $\mathrm{d}\sigma/\mathrm{d}y$ for ALICE, compared with results from other experiments, quoted when their p_T coverage extends to zero. Also in this case, a good agreement is found. It has to be noted that these results assume that J/ψ production is unpolarized. A direct measurement of J/ψ polarization, through the study of the angular distribution of the decay leptons, is currently underway and is extremely relevant for theory since models are not generally able to reproduce at the same time p_T distributions and polarization.

4. – Conclusions

After nearly twenty years of design, R&D, construction, installation, commissioning and simulations, the ALICE experiment is taking data since LHC started its operation at the end of 2009. Most systems have reached design performance, and several physics results are now available. Even if heavy-ion physics is the main subject, the experiment can also explore the LHC energy territory with pp collisions. The results, which have

been shortly outlined in this contribution, represent a fundamental reference for nuclear collision results [3] but also an interesting testing ground for QCD-related topics, from soft to semi-hard observables.

<div align="center">* * *</div>

The author would like to thank the organizers for the extremely pleasant and fruitful atmosphere of this workshop.

REFERENCES

[1] ALICE COLLABORATION, *J. Phys. G*, **30** (2004) 1517; **32** (2006) 1295.
[2] AAMODT K. *et al.* (ALICE COLLABORATION), *Eur. Phys. J. C*, **65** (2010) 111.
[3] DAINESE A. *et al.* (ALICE COLLABORATION), these proceedings.
[4] AAMODT K. *et al.* (ALICE COLLABORATION), *J. Instrum.*, **3** (2008) S08002.
[5] AAMODT K. *et al.* (ALICE COLLABORATION), *Eur. Phys. J. C*, **68** (2010) 89.
[6] AAMODT K. *et al.* (ALICE COLLABORATION), *Eur. Phys. J. C*, **68** (2010) 345.
[7] AAMODT K. *et al.* (ALICE COLLABORATION), *Phys. Lett. B*, **693** (2010) 53.
[8] AAMODT K. *et al.* (ALICE COLLABORATION), *Phys. Rev. Lett.*, **105** (2010) 072002.
[9] ROSSI G. C. and VENEZIANO G., *Nucl. Phys. B*, **123** (1977) 507.
[10] AAMODT K. *et al.* (ALICE COLLABORATION), *Eur. Phys. J. C*, **71** (2011) 1594.
[11] CACCIARI M., GRECO M. and NASON P., *JHEP*, **9805** (1998) 007; private communication.
[12] KNIEHL B. A. *et al.*, *Phys. Rev. Lett.*, **96** (2006) 012001; private communication.
[13] AAMODT K. *et al.* (ALICE COLLABORATION), *Phys. Lett. B*, **704** (2011) 442, arXiv:1105.0380.